Optical Materials 34 (2012) 1913–1916

Contents lists available at SciVerse ScienceDirect

Optical Materials

journal homepage: www.elsevier.com/locate/optmat

Femtosecond laser micromachining of Nd:GdCOB ridge waveguides for second harmonic generation

Yuechen Jia [a], Feng Chen [a,*], Javier R. Vázquez de Aldana [b], Sh. Akhmadaliev [c], Shengqiang Zhou [c]

[a] School of Physics, State Key Laboratory of Crystal Materials and Key Laboratory of Particle Physics and Particle Irradiation (MOE), Shandong University, Jinan 250100, China
[b] Laser Microprocessing Group, Universidad de Salamanca, Salamanca 37008, Spain
[c] Institute of Ion Beam and Materials Research, Helmholtz-Zentrum Dresden-Rossendorf, Dresden 01314, Germany

ARTICLE INFO

Article history:
Received 19 April 2012
Received in revised form 25 May 2012
Accepted 28 May 2012
Available online 23 June 2012

Keywords:
Optical waveguides
Nd:GdCOB laser crystal
Femtosecond laser micromachining
Second harmonic generation

ABSTRACT

We report on the fabrication of Nd:GdCOB ridge waveguides by using femtosecond laser micromachining of planar waveguides that were produced by carbon ion irradiation. The guiding properties of the Nd:GdCOB ridge waveguides are investigated. The second harmonic generation (SHG) at 532 nm green laser from ridges in a series of transverse widths is realized. The results show that the optical conversion efficiencies of SHG in the fabricated ridge waveguides are considerably enhanced with respect to the planar waveguide, and the maximum value reaches 11.4% under a pulsed 1064 nm laser pump.

1. Introduction

As one of the most promising gain media for self-frequency-doubling (SFD) lasers, the neodymium-doped gadolinium calcium oxoborate ($Nd:GdCa_4O(BO_3)_3$ or Nd:GdCOB) has attracted broad attention owing to the combination of excellent fluorescence features of incorporated Nd^{3+} ions and nonlinear properties of a GdCOB matrix [1–4]. Optical waveguides are the basic components in integrated photonics and modern telecommunication systems owing to the compact confinement of light propagation in extremely small volumes with dimensions of the order of several micrometers [5]. Benefiting from this advantage, much high optical intensity could be obtained in waveguides, and some improved performance, with respect to the bulks, could be achieved [6–8]. For example, it is expected that nonlinear waveguides allow the occurrence of diverse nonlinear phenomena at relatively low light powers. Particularly, for the crystals that serve as frequency converters, waveguide-based new frequency light generation could be with higher efficiency and more choice of different modes with respect to the bulks [7]. In practice, two dimensional (2D) waveguides (typically in channel or ridge configurations) are more attractive than one dimensional (1D) structures (such as planar and slab waveguides) due to the more compact geometry in 2D guiding structures and higher light intensity inside [9]. For oxoborate crystals, two techniques have been applied to fabricate 2D optical waveguide structures, i.e., ion implantation/irradiation [10–14], and ultrafast laser inscription [15]. Ion implantation/irradiation is a powerful method for waveguide construction, which has been proved successful in more than 100 materials [16–21]. The femtosecond (fs) laser micromachining has emerged as one of the most fascinating techniques owing to the widely practical applications for microfabrication of numerous materials [22–25]. In fact, the fs-laser ablation has been successfully applied to fabricate ridge waveguide structures on the surface of the β-BaB_2O_4 nonlinear planar waveguide [26]. Recently, we reported on the fabrication of planar waveguides in Nd:GdCOB crystals by 17 MeV C^{5+} ion irradiation, and efficient guided-wave SHG was realized in the 1D confinement configuration [12]. Even though, a 2D ridge waveguide is necessary to achieve higher-efficiency SHG and more compact geometry for integrated photonic devices. In this work, we report on the construction of ridge waveguides on the surface of 17 MeV C ions irradiated Nd:GdCOB planar waveguide by using the fs ablation, and the realization of SHG at ~532 nm in the ridge waveguide under a pulsed laser pump. The conversion efficiencies of SHG of the ridge waveguides with different scales are compared with the planar waveguides.

2. Experiments in details

Fig. 1a and b illustrate schematically the Nd:GdCOB ridge waveguide structures fabrication process. In the first step, the planar waveguide layer of ~11 μm was fabricated by 17 MeV carbon (C^{5+}) ions at a fluence of 2×10^{14} ions/cm^2 (details on the

* Corresponding author. Tel.: +86 531 88363007; fax: +86 531 88363350.
E-mail address: drfchen@sdu.edu.cn (F. Chen).

0925-3467/$ - see front matter © 2012 Elsevier B.V. All rights reserved.
http://dx.doi.org/10.1016/j.optmat.2012.05.032

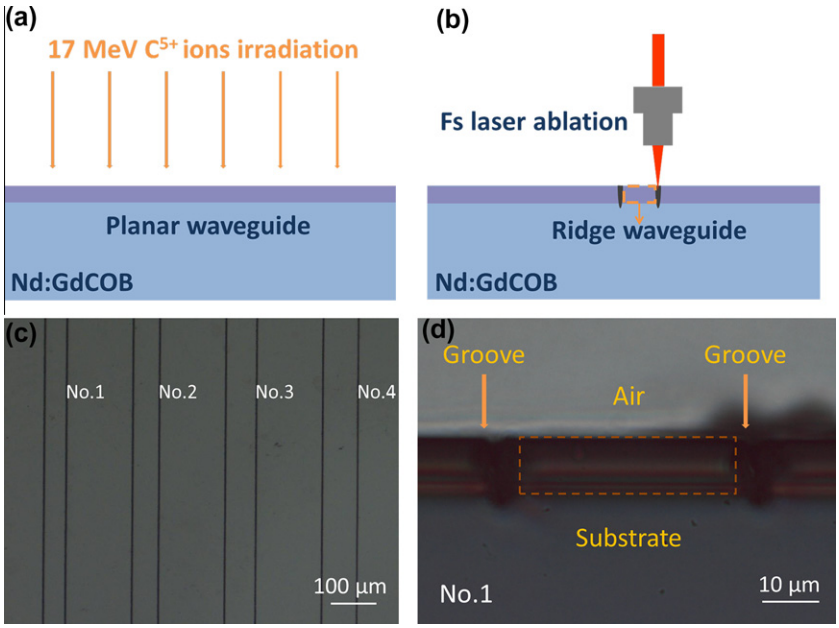

Fig. 1. The schematic of (a) 17 MeV C ions irradiation and (b) femtosecond laser ablation processes for the Nd:GdCOB ridge waveguide fabrication and the microscope image of the (c) surface and (d) end face of the ridge waveguides.

experiment can be found in [12]). Secondly, we used a Ti:Sapphire laser system, which delivered 120 fs pulses, linearly polarized at 796 nm and with a repetition rate of 1 kHz, to ablate parallel air grooves on the top of the ion irradiated planar waveguide surface to form the ridge waveguide. The laser beam was focused by a 20× microscope objective (NA = 0.4), and the sample was located at a XYZ motorized stage with a spatial resolution of 0.2 μm. The linear focus of the objective was located on the irradiated surface of the sample and the pulse energy was set to 2.1 μJ. As a consequence, multi-pair grooves were ablated, forming four ridge waveguides with diverse lateral width of 40 μm (No. 1), 50 μm (No. 2), 60 μm (No. 3) and 70 μm (No. 4) by scanning the sample with the laser at a translation velocity of 50 μm/s (see Fig. 1c for an image of the ridge waveguide sample surface). With the lateral confinement of microstructured grooves and vertical restriction of ion irradiated planar waveguide, the ridge waveguide structures were produced on the surface of Nd:GdCOB crystal. Fig. 1d shows the microscope image of the cross section of ridge waveguide No. 1 (the dashed line indicates the spatial location of the ridge waveguide structure) with a lateral separation of 40 μm. For comparison, about 1/4 of the surface layer is not microstructured, preserving the planar waveguide geometry.

We used scanning electron microscope (SEM) to study the roughness of the sidewalls of the fs-laser ablated ridge waveguides in Nd:GdCOB. Fig. 2a shows the surface topographic image of the ridge waveguide (No. 1). From the magnified SEM image (Fig. 2b), we could estimate the roughness of the sidewall to be ~1.8 μm.

The nonlinear performances of the waveguides were characterized by utilizing a typical end-face coupling system (see Fig. 3). For the SHG experiments of Nd:GdCOB waveguides, a pulsed laser beam at a wavelength of ~1064 nm, as the fundamental wave, was coupled into the waveguide by a convex lens with focal length f = 25 mm. The pulsed laser produced ~80 μJ pulses with a duration of 11.05 ns at a repetition of ~5 kHz, maximum average power of 480 mW. The light emerging from the output of the waveguides were captured by using a microscope objective lens (NA = 0.4). And the generated second harmonic (SH) light was separated from the leaked fundamental laser beam by using a mirror with transmission of ~70% at ~532 nm and reflectivity >99% at ~1064 nm, and then detected by the spectrometer, an infrared CCD camera and a powermeter. The coupling efficiency of the pump 1064 nm beam into the waveguides was determined to be averagely ~32%, which was calculated from the overlap of the pump beam and waveguide modal profiles.

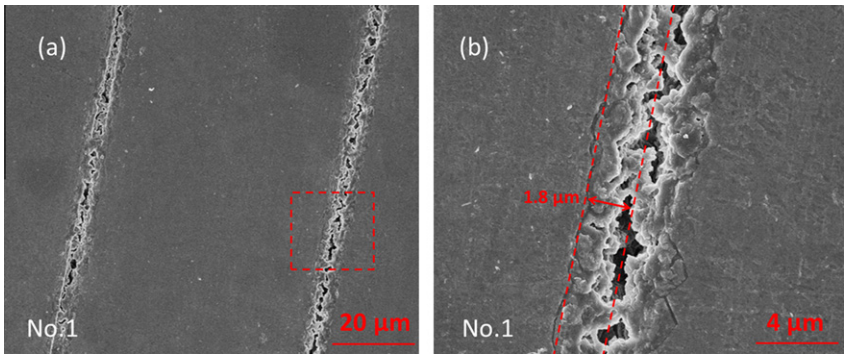

Fig. 2. The topographic SEM image of the of ridge waveguide No. 1, showing two adjacent grooves ablated on the Nd:GdCOB surface, and (b) the magnification of dashed line surrounded region in (a).

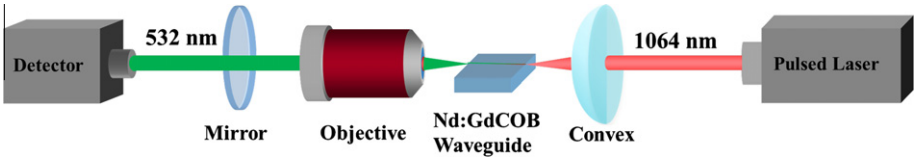

Fig. 3. Schematic of experimental arrangement for the SHG of Nd:GdCOB waveguides.

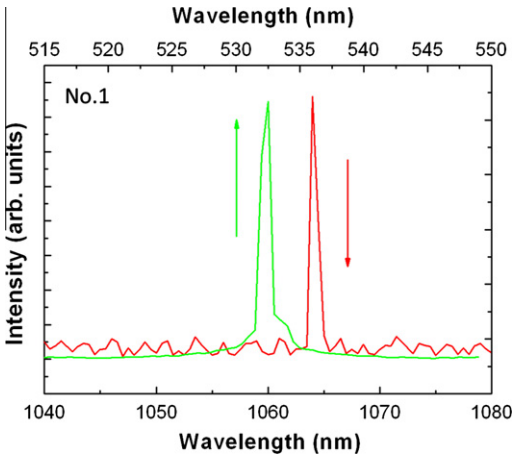

Fig. 4. Laser spectra of the fundamental (red) and SH (green) waves from the 40-μm wide Nd:GdCOB ridge waveguide produced by fs-laser micromachining of the planar waveguide. (For interpretation of the references to colour in this figure legend, the reader is referred to the web version of this article.)

3. Results and discussion

Fig. 4 depicts the typical laser spectra of the fundamental (at 1064 nm) and SH (at 532 nm) waves from the 40-μm wide Nd:GdCOB ridge waveguide under the pulsed laser pump configuration. The 1064-nm fundamental waves are with TM polarizations and the SH waves are with the TE one, i.e., the SHG process occurs under $TM^{\omega} \rightarrow TE^{2\omega}$, which is in accordance with the bulk SHG. It should be noted that for all the ridge waveguides and the planar waveguide studied in this work, the laser spectra for fundamental and SH waves are similar to those from the bulk, respectively, which suggests that the nonlinear properties of the crystal have been well preserved in the waveguide structures.

Fig. 5a–d shows the images of the fundamental modes (TM polarizations) of the ridge waveguides of Nos. 1–4, respectively. As one can see, the modal profiles depict zero-order modes, i.e., TM_0^{ω}. Compared with the planar waveguide mode (Fig. 5e), the lateral confinement by the fs-laser ablated grooves seems to be reasonable owing to the width of the constructed ridges. Fig. 5f–i display the SH guided modal images from the corresponding ridge waveguides. Since the SH waves at 532 nm are with a shorter wavelength than that of the fundamental ones, some of the SH modes are not in zero-order. In addition, as the ridge width increases, the SH mode resembles more like a planar waveguide (Fig. 5j). This is reasonable since the lateral confinement of the light between the two grooves plays less important role to balance the transverse diffraction of the light field. In the present work, the 40-μm wide ridge waveguide seems to be more advantageous because the fundamental and SH waves are both in zero-order modes, i.e., corresponding to the $TM_0^{\omega} \rightarrow TE_0^{2\omega}$ configuration SHG process.

Fig. 6a and b depict the generated SH wave powers (peak power of $P_{peak}^{2\omega}$ and mean power of $P_{mean}^{2\omega}$) at 532 nm as a function of the absorbed pump ones (peak power of P_{peak}^{ω} and mean power of P_{mean}^{ω}) of the 1064-nm fundamental waves for the 40-μm wide Nd:GdCOB ridge waveguide under the pulsed mode, respectively. The solid circles and the lines are the experimental data and the linear fit, respectively. The maximum output peak power of the SH light is ~110 W with a pump peak power of ~965 W, resulting in a conversion efficiency of $\eta_{peak} \approx 11.4\%$. Accordingly, the maximum output mean power of the SH light is ~5.4 mW with a pump mean power of ~111 mW, which corresponds to a conversion efficiency of $\eta_{mean} \approx 43.4\%\ W^{-1}$. It should be noted that for the ridges with different widths the conversion efficiency for 1064 → 532 nm SHG is different. Table 1 shows the measured maximum output power of SH guided light, the corresponding SHG conversion efficiency and the propagation loss from the ridge waveguides Nos. 1–4, respectively. For comparison, the data of the planar SHG is also included in the table.

As one can see from the table, as the ridge width increases from 40 to 70 μm (i.e., from Waveguide Nos. 1–4), the maximum powers of the SH guided light as well as the conversion efficiency decreases accordingly. In addition, compared with the planar waveguide, all the ridge waveguides possess higher conversion efficiency of SHG. This may be due to the more compact geometry of the ridge structures benefiting from the lateral confinement of the light fields, reaching higher optical intensities. Particularly, the conversion efficiency of the 40-μm wide ridge waveguide is

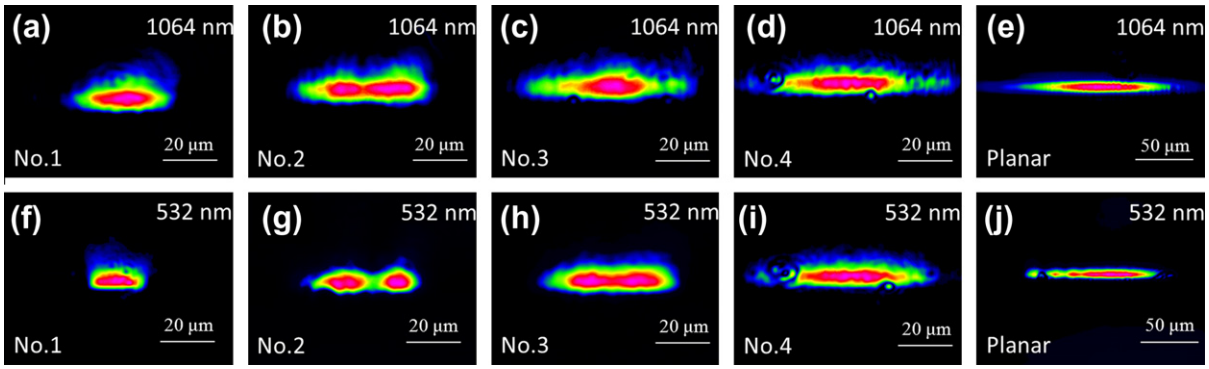

Fig. 5. Measured modal profiles of the fundamental (up, at 1064 nm) and SH (bottom, at 532 nm) waves of the ridge waveguides (Nos. 1–4) and planar waveguide.

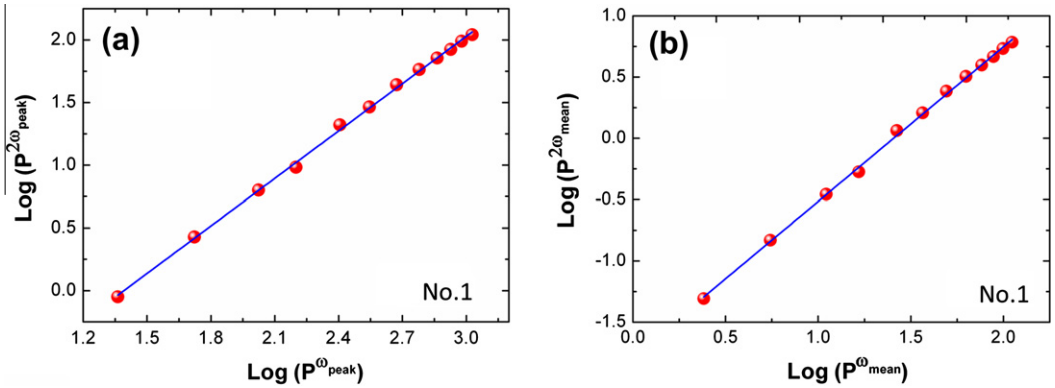

Fig. 6. The SH powers at ~532 nm as a function of the fundamental pump powers for the 40-μm wide ridge Nd:GdCOB waveguide: (a) in peak power and (b) in mean power.

Table 1
Maximum output SH powers ($P^{2\omega}$), 1064 → 532 nm SHG conversion efficiencies (η) and propagation losses (α) of the Nd:GdCOB ridge and planar waveguides.

	No. 1	No. 2	No. 3	No. 4	Planar
$P^{2\omega}_{peak}$ (W)	110	99	84	74	18
$P^{2\omega}_{mean}$ (mW)	5.4	4.9	4.2	3.7	0.9
η_{peak} (%)	11.4	10.5	9.5	9.2	4.6
η_{mean} (%W^{-1})	43.4	39.4	33.8	29.7	7.3
α (dB/cm)	6.7	6.1	6.0	5.7	5.1

2.5 times that of the planar waveguide, suggesting superior performance to the planar counterpart for guided-wave SHG. The propagation loss (α) of the ridge and planar waveguides at 632.8 nm are also shown in this table. We can find the loss value decreases as the ridge structure width increases, and the loss of the planar waveguide is the lowest (5.1 dB/cm). The higher attenuation for ridge waveguide should be partly attributed to the non-perfect sidewalls fabricated by the fs lasers, which brings out the additional attenuation through the scattering. It has been found that, for narrower ridges, the rough side walls affect the light propagation more obviously. After the annealing treatment at 260 °C for 1 h in the open air, the propagation loss values have no obvious changes, exhibiting good stabilities at moderate temperatures. From Table 1, one can also conclude that the SHG in ridge waveguide platform is superior to the planar waveguide, even if the propagation losses of the ridges are higher than that of the planar one. This reflects the fact that by using ridge waveguide to achieve 2D light confinement is an efficient method to improve the nonlinear SHG performance. One could expect even more advantageous SHG in narrower ridge Nd:GdCOB waveguide with more smooth side walls. It has been found that, ion beam sputtering may be a successful method to reduce the roughness of the side walls of the fs-laser ablated grooves of dielectric crystals (e.g., in β-BaB_2O_4 [26]) to reduce the propagation loss ridge waveguides. Future work would be focused on the improvement of guiding and SHG performance in the optimized Nd:GdCOB waveguide system by using similar techniques.

4. Conclusion

We have fabricated ridge waveguides in Nd:GdCOB crystals by using fs-laser micromachining of C ion irradiated planar waveguide. The SHG has been achieved through the ridge structures for the 1064 → 532 nm conversion. The results show that the fs-laser micromachined ridges are superior to the planar waveguides with considerable enhancement of SHG conversion efficiency. This work opens up a unique way to form ridge waveguides by combination of ion irradiation and fs-laser ablation in nonlinear crystals; as a result, versatile nonlinear applications may be expected by using such ridge waveguide configurations.

Acknowledgements

The work is supported by the National Natural Science Foundation of China (No. 10925524), the Spanish Ministerio de Ciencia e Innovación (MICINN) through Consolider Program SAUUL CSD2007-00013 and Project FIS2009-09522. S.Z. acknowledges the funding by the Helmholtz-Gemeinschaft Deutscher Forschungszentren (HGF-VH-NG-713). Support from the Centro de Láseres Pulsados (CLPU) is also acknowledged.

References

[1] G. Aka, A. Kahn-Harari, D. Vivien, J.M. Benitez, F. Salin, J. Godard, Eur. J. Solid State Inorg. Chem. 33 (1996) 726–736.
[2] G. Aka, A. Kahn-Harari, F. Mougel, D. Vivien, F. Salin, P. Coquelin, P. Colin, D. Pelenc, J.P. Damelet, J. Opt. Soc. Am. B 14 (1997) 2238–2247.
[3] C.Q. Wang, Y.T. Chow, W.A. Gambling, S.J. Zhang, Z.X. Cheng, Z.S. Shao, H.C. Chen, Opt. Commun. 174 (2000) 471–474.
[4] D. Vivien, F. Mougel, F. Augé, G. Aka, A. Kahn-Harari, F. Balembois, G. Lucas-Leclinm, P. Georges, A. Brun, P. Aschehoug, Opt. Mater. 16 (2001) 213–220.
[5] E.J. Murphy, Integrated Optical Circuits and Components: Design and Applications, Marcel Dekker, New York, 1999.
[6] D. Kip, Appl. Phys. B 67 (1998) 131–150.
[7] G.I. Stegeman, C.T. Seaton, J. Appl. Phys. 58 (1985) R57–R78.
[8] C. Grivas, Prog. Quant. Electron. 35 (2011) 159–239.
[9] F. Chen, Crit. Rev. Solid State Mater. Sci. 33 (2008) 165–182.
[10] A. Boudrioua, J.C. Loulergue, P. Moretti, B. Jacquier, G. Aka, D. Vivien, Opt. Lett. 24 (1999) 1299–1301.
[11] B. Vincent, A. Boudrioua, J.C. Loulergue, P. Moretti, S. Tascu, B. Jacquier, G. Aka, D. Vivien, Opt. Lett. 28 (2003) 1025–1027.
[12] Y.Y. Ren, Y.C. Jia, F. Chen, Q.M. Lu, Sh. Akhmadaliev, S.Q. Zhou, Opt. Express 19 (2011) 12490–12495.
[13] Y.Y. Ren, N.N. Dong, Y.C. Jia, L.L. Pang, Z.G. Wang, Q.M. Lu, F. Chen, Opt. Lett. 36 (2011) 4521–4523.
[14] Y.Y. Ren, Y.C. Jia, N.N. Dong, L.L. Pang, Z.G. Wang, Q.M. Lu, F. Chen, Opt. Lett. 37 (2012) 244–246.
[15] A. Rodenas, A.K. Kar, Opt. Express 19 (2011) 17820–17833.
[16] F. Chen, Laser Photon. Rev., doi: 10.1002/lpor.201100037.
[17] J. Olivares, G. García, A. García-Navarro, F. Agulló-López, O. Caballero, A. García-Cabañes, Appl. Phys. Lett. 86 (2005) 183501.
[18] G.B. Montanari, P. De Nicola, S. Sugliani, A. Menin, A. Parini, A. Nubile, G. Bellanca, M. Chiarini, M. Bianconi, G.G. Bentini, Opt. Express 20 (2012) 4444–4453.
[19] F. Chen, X.L. Wang, K.M. Wang, Opt. Mater. 29 (2007) 1523–1542.
[20] V.V. Atuchin, Nucl. Instrum. Methods Phys. Res. B 168 (2000) 498–502.
[21] S.M. Kostritskii, P. Moretti, Phys. Status Solidi (c) 11 (2004) 3126–3129.
[22] S. Juodkazis, V. Mizeikis, H. Misawa, J. Appl. Phys. 106 (2009) 051101.
[23] R.R. Gattass, E. Mazur, Nat. Photon. 2 (2008) 219–225.
[24] M. Ams, G.D. Marshall, P. Dekker, J. Piper, M. Withford, Laser Photon. Rev. 3 (2009) 535–544.
[25] F.M. Bain, A.A. Lagatsky, R.R. Thomson, N.D. Psaila, N.V. Kuleshov, A.K. Kar, W. Sibbett, C.T.A. Brown, Opt. Express 17 (2009) 22417–22422.
[26] R. Degl'Innocenti, S. Reidt, A. Guarina, D. Rezzonico, G. Poberaj, P. Gunter, J. Appl. Phys. 100 (2006) 113121.